RSC Advances

ROYAL SOCIETY OF CHEMISTRY

www.rsc.org/advances

Antibacterial properties of palladium nanostructures sputtered on polyethylene naphthalate

M. Polívková[a,*], M. Valová[a], J. Siegel[a], S. Rimpelová[b], T. Hubáček[c], O. Lyutakov[a] and V. Švorčík[a]

[a]*Department of Solid State Engineering, University of Chemical Technology Prague, 166 28 Prague, Czech Republic*

[b]*Department of Biochemistry and Microbiology, University of Chemical Technology Prague, 166 28 Prague, Czech Republic*

[c]*Institute of Hydrobiology, Biology Centre of the AS CR, 370 05 Ceske Budejovice, Czech Republic*

Abstract

Resistance of pathogenic bacteria to conventional antibiotics has emerged in recent years as a major problem for public health. In order to overcome this problem, non-conventional antimicrobial agents have recently been under investigation. Pd nanolayers of variable thicknesses ranging from 0.4 to 22.4 nm were prepared by sputtering on polyethylene naphthalate (PEN). Low-temperature annealing was applied to transform these nanolayers into discrete nanoislands homogeneously distributed over the surface of the underlying polymer. The antibacterial properties of these composites were evaluated by drip test using Gram-positive and Gram-negative bacteria as model strains. Inductively coupled plasma, X-ray photoelectron spectroscopy, and atomic force microscopy were used to outline the way of bacterial inhibition by Pd nanostructures. We found that the antibacterial effect of the Pd/PEN composites might be caused by both i) release of Pd into a physiological solution and ii) direct contact of bacteria with the Pd/PEN composites. Our results suggest that the samples coated with 22.4 nm thick Pd layer exhibited significantly enhanced antibacterial properties than the thinner Pd layers.

Keywords: Polyethylene naphthalate; Palladium; Sputtering; Annealing; Nanostructure; Antibacterial effect

[*]Corresponding author:

E-mail address: polivkoa@vscht.cz

1. Introduction

Biocompatible polymers are suitable materials for medical devices, such as catheters, endotracheal tubes, stents and prosthesis.[1-4] However, the use of untreated medical devices can lead to severe hospital-acquired infections. The most frequent types of these complications are pneumonia, surgical site infection, urinary tract and bloodstream infection, all of which are very often caused by Gram-negative bacteria.[5]

Several studies have demonstrated the antibacterial effects of a broad scale of compounds, both organic and inorganic, attached to polymer-based medical devices. For instance, quaternary ammonium[6] and hydantoin compounds,[7] chitosan,[8] and silver[9] have all been used in this regard.

The antibacterial effects of palladium[10] appear to be particularly interesting. Pd(II) complexes (Schiff-bases) were examined for the ability to inhibit both Gram-positive (*B. subtilis* and *S. aureus*) and Gram-negative (*E. coli* and *K. pneumonia*) bacteria and the minimum inhibitory concentration was determined. These complexes showed an excellent capability to fight the bacterial strains; their efficiency even being comparable to standard drugs, such as streptomycin and ampicillin.[10] In another study, the minimum inhibitory concentration of Pd(II) complexes with tetracycline was determined using *E. coli* as a model organism. These palladium-tetracycline complexes were 16 times more active than tetracycline itself. *E. coli* was, however, fully resistant to separate tetracycline treatment.[11] The agar well diffusion method was used to test the antibacterial effects of Pd(II) dithiocarbamates against six bacterial strains (*E. coli*, *B. subtilis*, *S. flexneri*, *S. aureus*, *S. typhi*, and *P. aeruginosa*). Metal complexes containing piperidine, 4-methylpiperridine and N-methylbenzylamine demonstrated high antibacterial potency, while complexes of dicyclohexyldithiocarbamate and N-cyclohexyl-N-methyldithiocarbamate demonstrated weak antibacterial activity, except against *S. flexneri*.[12]

Various methods have been used to investigate the antibacterial effects of Pd nanoparticles (Pd NPs). When the antibacterial circle method was used to expose *E. coli* to Pd-doped titanium nanoparticles, the Pd-doped samples exhibited stronger antibacterial response compared to pristine ones.[13] Trypic soy plates were also used to examine the antibacterial effects of Pd NPs against Gram-negative bacteria *E. coli* and Gram-positive bacteria *S. aureus*. Surprisingly, *S. aureus* was inhibited by remarkably low concentrations of Pd NPs, while the growth of *E. coli* was completely unaffected.[14] The antibacterial effect of Pd and Pt NPs was studied by drip method using *E. coli* and *S. epidermidis* as model organisms. Unlike Pt NPs, Pd NPs displayed an excellent response against both microorganisms.[15]

Despite the above described evidence that Pd, and more specifically Pd NPs, is an excellent antibacterial agent, no comprehensive study has yet been published on the application of Pd in

antibacterial coatings for medical technology. Thus, we investigated the antibacterial response of nanostructured Pd coatings supported on the type of polymer carriers used in medical instrumentation. Our approach is based on the low-temperature transformation of Pd nanolayers into discrete nanoislands. As a substrate we used polyethylene naphthalate (PEN) due to its excellent resistance against chemicals, high temperature, and mechanical stress. Surface characterization of the Pd/PEN composites, both before and after thermal annealing was studied by atomic force microscopy (AFM) and correlated with their antibacterial properties.

2. Experimental

2.1. Materials, apparatus and procedures

Polyethylene naphthalate foil (PEN, thickness 50 μm, density 1.36 $g \cdot cm^{-3}$) supplied by Goodfellow Ltd., UK was used in this work. Pd coatings were performed on diode sputtering system BAL-TEC SputterCoater SCD 050 with 99.999 % pure palladium target (Goodfellow Ltd., UK). The parameters of the deposition were: room temperature (20°C), current of 15 mA, total argon pressure of 5 Pa (gas purity 99.99 %), and electrode distance of 50 mm. Sputtering times varied from 10-200 s; samples (Ø 1 cm) were prepared during each deposition. Sample annealing was conducted in a thermostat Binder oven in air atmosphere at 250°C for 1 h. After this, the samples were cooled down in air and stored under laboratory conditions.

2.2. Analytical methods

Surface morphology and roughness of pristine and Pd-coated samples (both as-sputtered and annealed) were examined by AFM VEECO CP II device in a tapping mode. Surface roughness, characterized by the mean roughness value (R_a), represents the arithmetic average of the deviation from the centre plane of a sample.

Effective thicknesses of Pd layers were determined on the same AFM device by scratch method using Bruker Antimony-doped Silicon probe CONT20A-CP with the spring constant 0.9 $N \cdot m^{-1}$. We use a glass substrate, simultaneously coated with PEN samples, on which the thickness of deposited Pd was determined.

For the determination of the electrical sheet resistance (R_s) of the palladium layers before and after annealing, the standard Ohm`s method using KEITHLEY 487 pico-ampermeter was used. The range of the sputtering times was carefully chosen to cover all of the typical growth stages of the layers (discontinuous, transition area, continuous layer).Two additional Pd contacts (about 50 nm thick) were sputtered on the layer surface for R_s measurement. Typical error of the measurement was 5 %.

The atomic concentrations of palladium Pd(3d), carbon C(1s) and oxygen O(1s) in pristine PEN and Pd/PEN samples were studied by X-ray photoelectron spectroscopy (XPS) on Omicron Nanotechnology ESCAProbeP spectrometer. We used the X-ray source, which was monochromated at 1486.7 eV with a step size of 0.05 eV. The evaluation of spectra was performed by CasaXPS software.

For the partial removal of the surface, the *in situ* ablation of Pd-coated samples (both as-sputtered and annealed) was carried out by Ar^+ ions (acceleration voltage 1.2 keV) for 5 min on the same Omicron Nanotechnology ESCAProbeP spectrometer; the elemental concentrations in ablated samples were determined. The samples were studied under the electron take-off angles of 0° and 81°.

Inductively coupled plasma with mass spectroscopy detector (ICP-MS) was used to determine the amount of Pd ions released into physiological solution during the same conditions as antibacterial testing. The trace element analysis of Pd leachates was conducted by using Agilent 8800 triple-quadrupole spectrometer (Agilent Technologies, Japan) connected to auto-sampler. Sample nebulisation was performed using a MicroMist device equipped with a peristaltic pump. To minimize the interference of analyte with possible adducts (CrCr, CuAr, GeCl, ZnCl) we used a collision cell (He collision gas) operating in a high-energy mode. The uncertainty of measurement was less than 3 %. The leachates were prepared under the same conditions as the drip antibacterial test (see below); 1 ml of sterile physiological solution (PS, 0.9 % NaCl) was left in the contact with the tested samples (as-sputtered and annealed) under both static and dynamic (shaking at 130 rpm) conditions. The leachates were analyzed after 3 and 24 h of incubation.

2.3. Antibacterial tests

Antibacterial properties of pristine PEN and Pd/PEN composites (as-sputtered and annealed) were examined statically and dynamically by the drip test using two environmental bacterial strains; Gram-negative bacteria *Escherichia coli* (*E. coli*, DBM 3138) and Gram-positive bacteria *Staphylococcus epidermidis* (*S. epidermidis*, DBM 3179). *E. coli* was cultivated in Luria-Bertani broth medium (LB) and on LB agar plates. *S. epidermidis* was cultivated in Plate count broth (PCA broth) and on Plate count agar (PCA) plates. The inocula of both bacterial strains were prepared by overnight cultivation in orbital shaker at 37°C, then the optical densities were measured at 600 nm. The starter inocula were prepared by dilution of the overnight cultures in sterile physiological solution (PS). Tested samples were immersed in 1 ml of PS and were inoculated with *E. coli* (1.1×10^4 of colony forming units from a single bacterial cell (CFU) per 1 ml) and with *S. epidermidis* (2.2×10^4 of CFU per 1 ml). In parallel, *E. coli* and *S. epidermidis* incubated solely in

PS were used as positive controls. The samples were incubated under both static and dynamic (shaking at 130 rpm) conditions at 24°C for 1 h. Afterwards, aliquots of 25 µl from each vigorously vortexed sample were placed on pre-dried agar plates (LB agar, PCA) in 10-fold repetitions. Each sample was tested in a triplicate. After 3 and 24 h of incubation at 24°C (*E. coli*) and 37°C (*S. epidermidis*), the number of CFU was counted. The experiments were accomplished under sterile conditions.

3. Results and discussion

This section is divided into three parts: (i) surface characterization, (ii) surface ablation and Pd release, and (iii) antibacterial testing. In the surface characterization section, we used AFM-scratch method to measure the effective thicknesses of the prepared layers; surface morphology was carried out by AFM; electrical continuity of Pd layers was determined by the sheet resistance (R_s) measurements; chemical composition of the samples (original and ablated surface) was studied by XPS which provided atomic concentrations of individual elements. The antibacterial properties were studied in a static and dynamic mode by the drip test using two common microorganisms: *E. coli* (naturally occurring on mucous membranes) and *S. epidermidis* (human skin). Thereafter, the way of antibacterial growth inhibition mechanism was studied. We performed the ICP-MS analysis of the Pd leachates to determine the release of Pd into PS.

3.1. Surface characterization

The effective thicknesses of Pd nanolayers were examined for the sputtering times of 10-200 s (see Fig. 1). We found purely linear relationship between the effective thickness and sputtering time with uncertainty less than 1 %, which indicates strictly proportional sputtering rate. Nevertheless, this phenomenon is dissimilar to effective thicknesses measurement of Ag layers,[16] in which two constant but different deposition rates were found.

The measurement of sheet resistance (R_s) was used to determine the electrical continuity of thin Pd coatings. The dependence of R_s of Pd layers on the deposition time before and after annealing is shown in Fig. 2. For the as-sputtered samples, the R_s decreased rapidly in the narrow range of the deposition times from 60–140 s when an electrically continuous Pd layer was formed. The resulting R_s is saturated at the level of ca 140 Ω, which is the typical value of R_s in case of nanometer scale metal coatings (Matthiessen's rule).[17] For the annealed samples, one can see a significant shift of the resistance curve towards longer sputtering times (thicker coatings) which is in accordance with the transformation of the structure into isolated Pd nanoislands determined by AFM (see Fig. 3). The annealed samples were electrically discontinuous up to the sputtering time of 160 s (Pd

effective thickness of 17.8 nm) above which a percolation limit was overcome and the continuous layer was formed. For the higher sputtering times up to 500 s, the R_s decreased gradually and it achieved saturation at the same level which was observed on the as-sputtered layers. As the representatives of electrically discontinuous and continuous layers (R_s measurements), the samples of the sputtering times of 20 and 200 s were chosen for following analyses, respectively.

The surface morphology of pristine and Pd-coated samples both as-sputtered and annealed was characterized by surface roughness (R_a) measurements and three-dimensional AFM scans (see Fig. 3). Surface morphology of pristine PEN and as-sputtered samples exhibited only mild corrugation and the surface roughness had practically the same value regardless of specific thickness of Pd coating. No significant changes in surface morphology occurred after the annealing neither in the case of pristine polymer nor the Pd coated samples (deposition time 20 s). Contrary to that, we have observed a remarkable change in the case of a thicker layer (deposition time 200 s); the annealing resulted in a complete rearrangement of the surface. This might be caused by thermally induced changes in the amorphous phase of PEN (T_g^{PEN} = 120°C) as a result of thermal accumulation in a thicker metal coating. This dramatic change in surface morphology resulted in a significant increase of R_a, which was augmented by two orders of magnitude compared to as-sputtered samples. The change in morphology, which was apparent especially for the annealed samples of 200 s, represents the transformation of continuous coating (see Fig. 2) into isolated Pd islands homogeneously distributed over the polymer surface. This phenomenon was supported by XPS measurements (see Tab. 1); the amount of Pd after annealing was reduced at the expense of the amount of elements originating from PEN. It is evident that the size of the Pd islands might be effectively controlled by the thickness of Pd coating preceding the annealing process. The formation of island-like structures led to increase of surface area, which might result in enhanced antibacterial response. In several different studies, the formation of island-like structures after annealing was detected in case of silver[16] and gold coatings.[18]

Atomic concentrations, determined from XPS spectra for pristine, as-sputtered, and annealed samples, are summarized in Tab. 1. Typical accessible depth of XPS is up to ten atomic layers beneath the sample surface. The concentrations of C and O originate from PEN stoichiometry and might be shifted in favour of C due to adsorbed hydrocarbon impurities. Hydrocarbon impurities are ordinarily found on the surfaces of polar materials such as PEN and they are mostly adsorbed from air.[19] We found that the detected amounts of Pd increased with the thicknesses of the Pd layer (for both as-sputtered and annealed samples). After annealing, however, the detected concentration of Pd decreased at the expense of the concentration of elements originating from the underlying polymer, most likely due to diffusion and aggregation of Pd (see Fig. 3). The relatively high value

of the atomic concentration of O for the annealed samples of 20 s could be explained by higher propensity for oxidation of the thinner layers during annealing, which was confirmed by deconvolution of Pd peak and by assigning the proper oxidation states to Pd.

3.3. Surface ablation and Pd release

In order to outline the principle of bacterial inhibition, the as-sputtered and annealed samples (deposition time 200 s) were studied also after ablation performed *in situ* in an XPS chamber. The experimental arrangement allowed detection of electrons under take-off angles of 0 and 81° (see Tab. 2). When measuring in electron take-off angle of 0°, the analyte information originates from perpendicular direction to the sample surface, thus the information about the chemical composition comes from a greater depth compared to wide angle detection (electron take-off angle of 81°, lower depth information).[20] The concentration of Pd in the as-sputtered samples increased after the ablation for both angles (0° and 81°), which indicates that the hydrocarbon impurities were partially removed from the surface. Significant decrease in the concentration of O after ablation also gave the evidence of the presence of oxidized hydrocarbon (C-O type) impurities. While the as-sputtered samples (deposition time 200 s) were electrically continuous with apparently flat morphology (see Figs. 2 and 3), the annealed samples exhibited electrically discontinuous layer with island-like structures (see Figs. 2 and 3). However, in the light of XPS results, we attribute the changes in the surface morphology not only to the coalescence of Pd into separate nano-islands, but also to embedding of these clusters into the polymer interior. This incorporation is, however, very superficial most likely reminding ultrathin (ones of nm) polymer overlay reaching almost the top of individual Pd-islands (a "curtain" effect, see Fig. 4). The key information for understanding the transformation of the surface is provided by XPS data in Tab. 2; the ablation of the annealed sample showed that the concentration of Pd decreased, when we change the electron take-off angle from 0° (a higher depth) to 81° (a lower depth). This phenomenon was marginal in case of as-sputtered samples, where one can expect continuous coverage of the polymer by metal (see Figs. 2 and 3). Slight fluctuation of Pd concentration is probably caused by irregularity of the surface which is not perfectly planar. The insertion of Pd clusters into the polymer induced by annealing had a significant impact on resulting antibacterial activity. Although the specific surface area of Pd was increased, there was no improvement in resulting antibacterial properties due to the "curtain" effect. The higher concentration of O in the annealed samples (originating from PEN) contrary to the as-sputtered samples (-C-O- impurities) and the higher concentration of Pd in the annealed samples after ablation (removal of the polymer coverage from Pd islands) is also in accordance with the above-mentioned phenomenon.

The concentrations of Pd in 3 h and 24 h leachates measured by ICP-MS are summarized in Tab. 3. The release of Pd from the as-sputtered and annealed samples into PS was carried out in the static and dynamic mode. We found that the concentrations of released Pd were almost independent on the specific method employed (static or dynamic, see Tab. 3). Due to this phenomenon, the differences between static and dynamic antibacterial tests results (see Figs. 7 and 8) might be caused only by the differences between static and dynamic contact of bacteria with the sample surface. In both, static and dynamic leachates, the concentration of Pd increased with the leaching time in case of all measured samples. Effective thicknesses of Pd layers correspond with the detected concentrations of Pd in the leachates; it increased with the effective thickness. Lower concentrations of Pd in the leachates from the annealed samples compared to the leachates from the as-sputtered samples (samples of 20 and 200 s) are in good accordance with the phenomenon of above described "curtain" effect (see Fig. 4) and with resulting lower antibacterial strength of the annealed samples (see Figs. 7 and 8).

In order to find out in which form the Pd is released into the solution, separation of XPS spectra of as-sputtered sample (deposition time 200 s) was conducted (see Fig. 5). From the shape of original Pd doublet (3d3/2 and 3d5/2) it is obvious that the signal envelope is superimposed from two peeks; dominant one belonging to metal Pd in ground oxidation state Pd^0, and much smaller one which may be attributed to higher oxidation states of Pd (Pd^{x+}). However, owing to the charging effect during XPS measurement of ultra-thin Pd layer, it is difficult to distinguish the exact Pd oxidation state. Since oxidized forms of palladium are easily soluble in water,[21] one can expect the Pd in the leachates originates predominately from dissolution of its oxidized form. The Pd^{x+}/Pd^0 ratio (calculated form the ratio of corresponding peaks area from XPS spectra) is 4/100, thus, only 4 % of Pd is supposed to be released during the antibacterial testing. This amount corresponds well with the concentration of Pd measured by ICP-MS. Therefore, one can expect Pd in the leachates is predominantly in the form of Pd ions.

3.2. Antibacterial tests

Another aim of this study was to assess the bactericidal activity of the Pd/PEN composites. The antibacterial properties of these composites were evaluated by drip method using Gram-negative bacteria of *E. coli* and Gram-positive *S. epidermidis*. The bacteria were in direct contact with the tested materials in physiological solution either under static or dynamic conditions for 3 and 24 h and then inoculated on solid agar plates. The inhibition effect of Pd-coated PEN as-sputtered for 200 s after 3 h in contact under static incubation conditions is depicted in Fig. 6 showing bacterial

colonies of *E. coli* growing on an LB agar plate: positive control on the left, PEN/Pd/200 s on the right.

From Fig. 7, it is apparent that after 3 h, the Pd/PEN composites had the most antibacterial activity against *E. coli* after the longest deposition time of 200 s under both static and dynamic conditions. Interestingly, as-sputtered PEN/Pd/200s samples incubated statically in PS totally inhibited growth of *E. coli.* However, when incubated dynamically, both as-sputtered and annealed PEN/Pd/200s samples had the same potency against *E. coli.* After 24 h, the most potent bactericidal activity was observed also for as-sputtered and annealed PEN/Pd/200s samples.

Very interestingly, *S. epidermidis* as a member of Gram-positive bacteria was more susceptible to PEN/Pd composites. From Fig. 8 it is clear that already samples as-sputtered for 20 s had a significant effect on suppression of bacterial growth after 3h cultivation under static conditions. After 24 h, the effect was even more pronounced. Similarly as for *E. coli*, the thickest Pd layer (samples as-sputtered or annealed for 200 s) inhibited growth of *S. epidermidis* after both 3 and 24 h in contact.

The antibacterial activity of PEN/Pd composites was proportional to the thickness of a Pd nanolayer; the thicker the layer, the stronger the antibacterial response. Thus, the most significant inhibition of bacterial growth was observed for PEN samples coated with a Pd layer of 22.4 nm thick (samples as-sputtered or annealed for 200 s). Overall, the bactericidal activity of these PEN/Pd composites could be caused by (i) close contact of bacteria with the surface (ii) release of Pd or Pd ions from the surface.

4. Conclusions

We have introduced a versatile and relatively simple approach for the creation of permanent bactericidal coatings on PEN foil. The preparation processes were successfully optimized to ensure the strong antibacterial effect of Pd nanostructures in the form of both layers and nanoislands. Systematic surface characterization enabled us to propose the mechanism by which the annealed surface transforms: Pd tends to aggregate while at the same time is covered with a thin polymer layer. The combination of XPS and ICP-MS provided detailed information about the transformation of the layers and broadened our understanding of the bacteria inhibition effect. Due to these measurements, we may attribute the nature of antibacterial action to the contact of bacteria with metal Pd and the release of Pd ions into a physiological solution. However, although it was not possible to fully determine which phenomenon predominates, we believe that the presented results provide a good basis for the application of these newly developed composites in medicinal technology. The Pd coatings introduced here appear to be stable antibacterial coatings for the

temperature-resistant and biocompatible polymers used in medical devices. These nanostructures are also potentially applicable to tissue engineering for antibacterial treatment in the artificial replacement of the outer skin layer. To provide further insight into the process of bacterial suppression we will next focus on a deeper examination of the mechanism of the antibacterial action of Pd.

Acknowledgements

Financial support of this research from the GACR projects Nos. 14-18131S, 15-19485S, and from the Ministry of Health of CR No. 15-33018A is gratefully acknowledged.

References

1 D. S. Jones, D. W. J. McLaughlin, C. P. McCoy and S. P. Gorman, *Biomaterials*, 2005, **26**, 1761.

2 A. Dodge-Khatami, H. W. M. Niessen, L. H. Koole, M. G. Klein, T. M. van Gulik and B. A. J. M. de Mol, *Asian Cardiovasc. Thorac. Ann.*, 2003, **11**, 245.

3 A. L. Lewis, L. A. Tolhurst and P. W. Stratford, *Biomaterials*, 2002, **23**, 1697.

4 T. Moro, Y. Takatori, K. Ishihara, T. Konno, Y. Takigawa, T. Matsushita, U. Chung, K. Nakamura and H. Kawaguchi, *Nat. Mater.*, 2004, **3**, 829.

5 R. Gaynes and J. R. Edwards, *Clin. Infect. Dis.*, 2005, **41**, 848.

6 J. Lin, S. Qiu, K. Lewis and A. M. Klibanov, *Biotechnol. Bioeng.*, 2002, **83**, 168.

7 Y. Sun and G. Sun, *J. Appl. Polym. Sci.*, 2003, **88**, 1032.

8 A. H. Greene, J. D. Bumgardner, Y. Yang, J. Moseley and W. O. Haggard, *Clin. Orthop. Rel. Res.*, 2008, **466**, 1699.

9 K. K. Lai and S. A. Fontecchio, *Am. J. Infect. Control*, 2002, **30**, 221.

10 B. Geeta, K. Shravankumar, P. M. Reddy, E. Ravikrishna, M. Sarangapani K. K. Reddy and V. Ravinder, *Spectrochim. Acta, Part A*, 2010, **77**, 911.

11 W. Guerra, E. D. Azevedo, A. R. D. Monteiro, M. Bucciarelli-Rodriguez, E. Chartone-Souza, A. M. A. Nascimento, A. P. S. Fontes, L. Le Moyec and E. C. Pereira-Maia, *J. Inorg. Biochem.*, 2005, **99**, 2348.

12 F. Shaheen, A. Badshah, M. Gielen, M. Dusek, K. Fejfarova, D. de Vos and B. Mirza, *J. Organomet. Chem.*, 2007, **692**, 3019.

13 Z. Jing, Ch. Wang, G. Wang, W. Li and D. Lu, *J. Sol-Gel Sci. Techn.* 2010, **56**, 121.

14 C. P. Adams, K. A. Walker, S. O. Obare and K. M. Docherty, *PLoS One*, 2014, **9**, 1.

15 M. Staszek, J. Siegel, K. Kolarova, S. Rimpelova and V. Svorcik, *Micro & Nano Letters* 2014, **9**, 778.

16 J. Siegel, P. Juřík, Z. Kolská and V. Švorčík, *Surf. Interface Anal.*, 2013, **45**, 1063.

17 K. L. Chopra, Thin Film Phenomena, McGraw Hill, New York 1969.

18 J. Siegel, R. Krajcar, Z. Kolská, V. Hnatowicz and V. Švorčík, *Nanoscale Res. Lett.*, 2011, **6**, 1.

19 K. B. Lewis and B. D. Ratner, *J. Colloid Interf. Sci.*, 1993, **159**, 77.

20 B. J. Tyler, D. G. Castner and B. D. Ratner, *Surf. Interface Anal.*, 1989, **14**, 443.

21 M. Gregory, *Johnson Matthey Technol. Rev.*, 2014, **58**, 212.

Table 1

Atomic concentration of C(1s), O(1s) and Pd(3d) measured by XPS (pristine PEN, as-sputtered and annealed samples coated by Pd)

Sample	**Sputtering time** (s)	**Atomic concentrations of elements** (at. %)		
		C	**O**	**Pd**
As-sputtered	0	84.1	15.9	-
	20	82.3	15.1	2.6
	200	73.5	1.2	25.3
Annealed	0	73.1	26.9	-
	20	73.6	25.1	1.3
	200	65.6	18.3	16.1

Table 2

Atomic concentration of C(1s), O(1s) and Pd(3d) measured by XPS (as-sputtered and annealed samples of 200 s) before and after ablation, electron take-off angle of 0 and 81°

Sample	**Ablation time** (min)	**Angle** (°)	**Atomic concentrations of elements** (at. %)		
			C	**O**	**Pd**
As-sputtered	0	0	73.5	1.2	25.3
	0	81	76.2	-	23.8
	5	0	53.3	1.1	45.6
	5	81	47.5	-	52.5
Annealed	0	0	65.6	18.3	16.1
	0	81	79.6	16.8	3.6
	5	0	66.7	8.6	24.7
	5	81	81.9	13.2	4.9

Table 3

Concentration of Pd ($ng \cdot ml^{-1}$) in static/dynamic leachates measured by ICP-MS (as-sputtered and annealed samples coated by Pd)

Sample	**Sputtering time** (s)	**Concentrations of Pd** ($ng \cdot ml^{-1}$)	
		3 h	**24 h**
As-sputtered	20	0.7 / 0.5	3.6 / 3.2
	200	1.5 / 1.3	5.5 / 5.9
Annealed	20	0.1 / 0.1	0.3 / 0.3
	200	0.6 / 0.4	2.4 / 2.1

Figure captions

Fig. 1

Dependence of the effective thickness of Pd layers on sputtering time.

Fig. 2

Dependence of the electrical sheet resistance (R_s) on the sputtering time of Pd for the as-sputtered and annealed samples.

Fig. 3

3D AFM images of pristine and Pd-coated PEN (sputtering time 20 and 200 s) before (As-sputtered) and after annealing (Annealed).

Fig. 4

Scheme of PEN processing resulting in "curtain" effect: (A) pristine PEN, (B) PEN sputtered with Pd, and (C) coalescence of Pd after annealing with detail view.

Fig. 5

Separation of XPS spectra of Pd (3d3/2 and 3d5/2 peaks, Pd^0 - ground oxidation state, Pd^{x+} - higher oxidation states) belonging to as-sputtered sample (deposition time 200 s, electron take-off angle 0°).

Fig. 6

Photograph showing the inhibition effect of Pd-coated PEN on *E. coli*. Bacterial colonies growing on LB agar plate: (A) positive control, (B) *E. coli* treated with Pd-coated PEN (as-sputtered sample of 200 s after 3 h static leachate).

Fig. 7

Dependence of number of CFU for *E. coli* on sputtering time for pristine and Pd-coated PEN in 3 h leachate (A) and 24 h leachate (B). Horizontal lines represent reference level (number of CFU in physiological solution) together with its uncertainty (dash line).

Fig. 8

Dependence of number of CFU for *S. epidermidis* on sputtering time for pristine and Pd-coated PEN in 3 h leachate (A) and 24 h leachate (B). Horizontal lines represent reference level (number of CFU in physiological solution) together with its uncertainty (dash line).

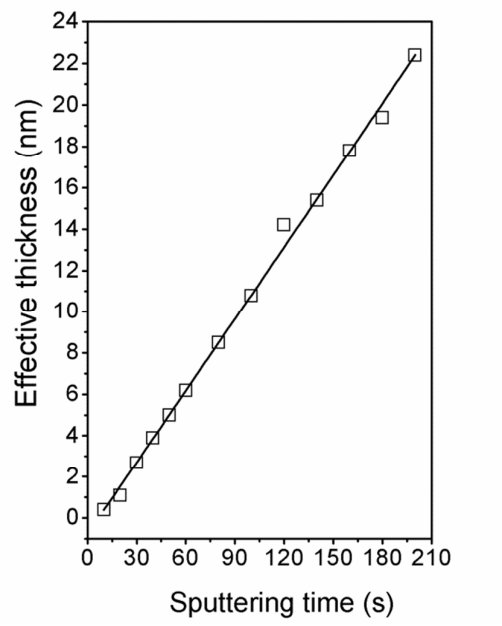

Fig. 1

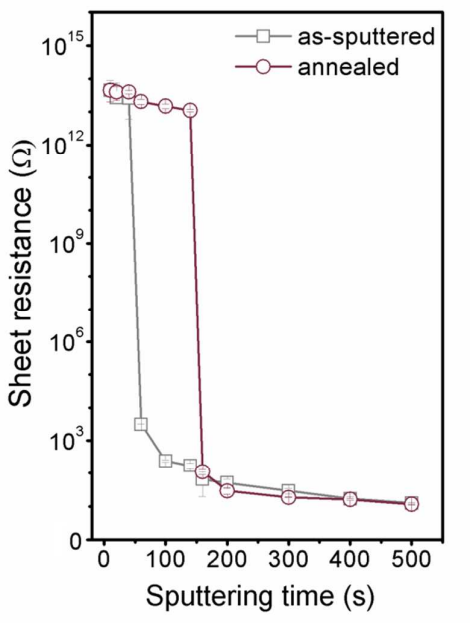

Fig. 2

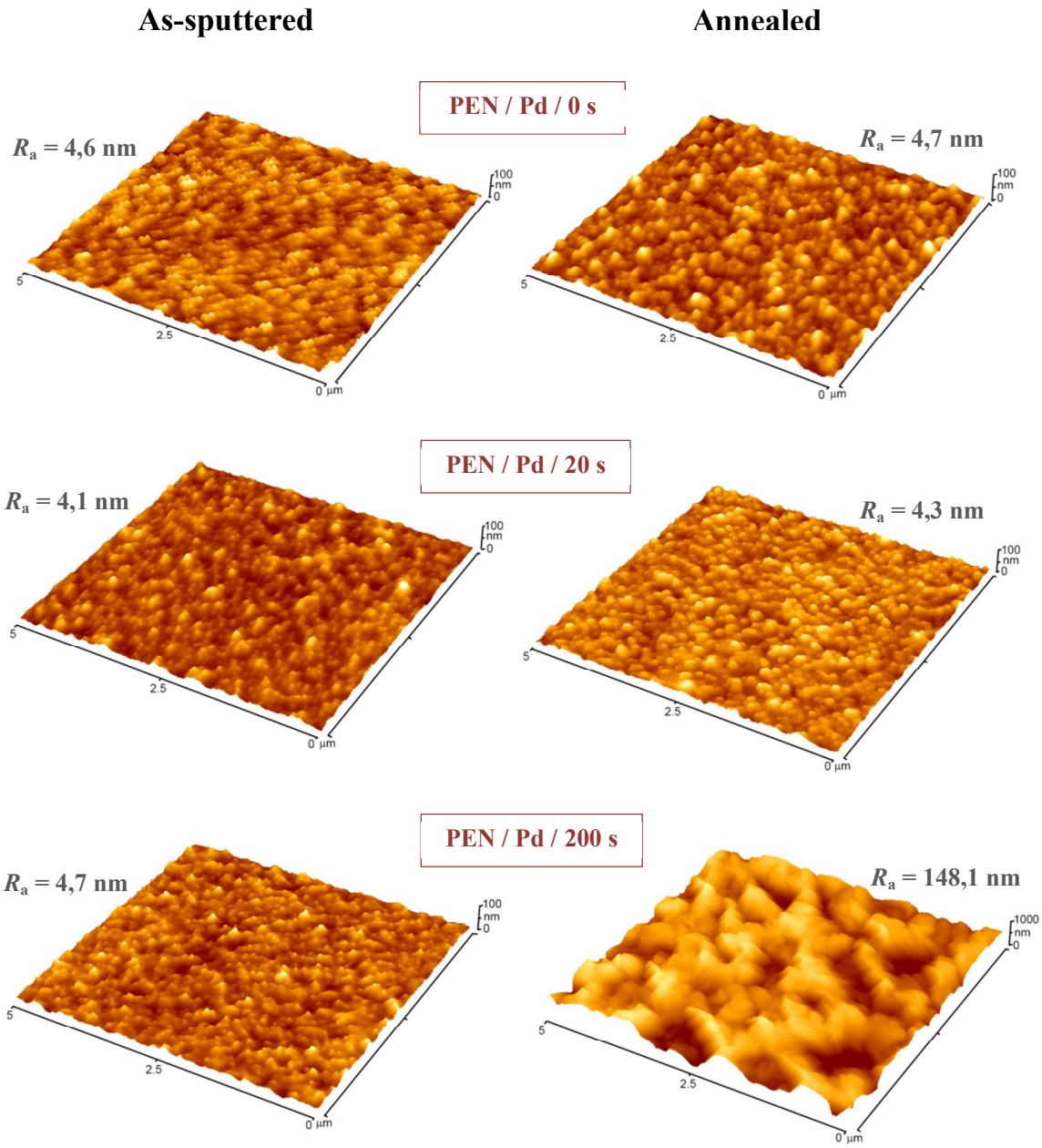

Fig. 3

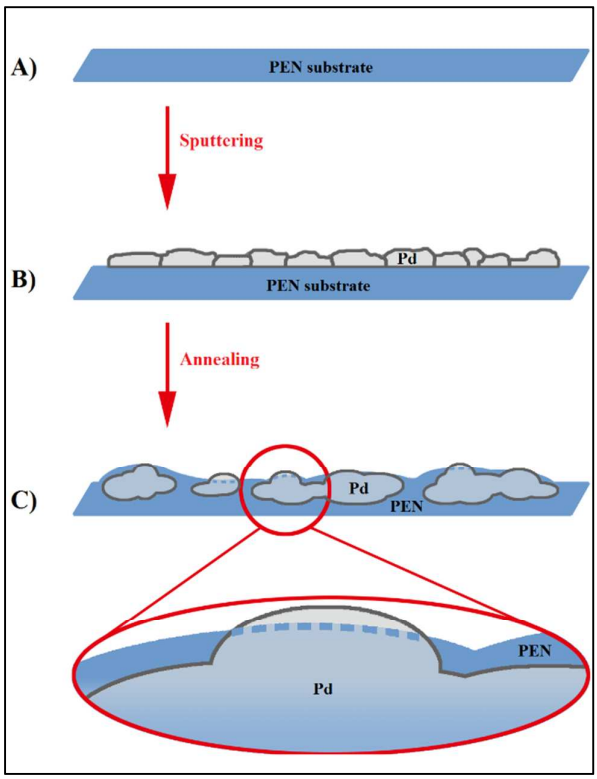

Fig. 4

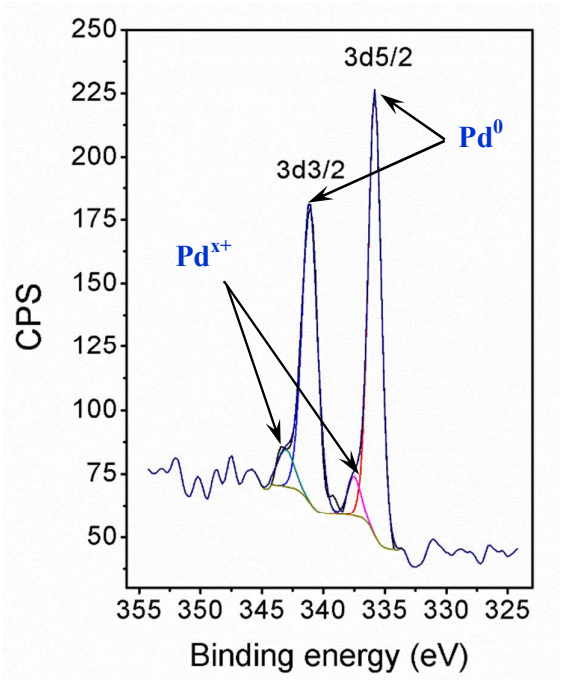

Fig. 5

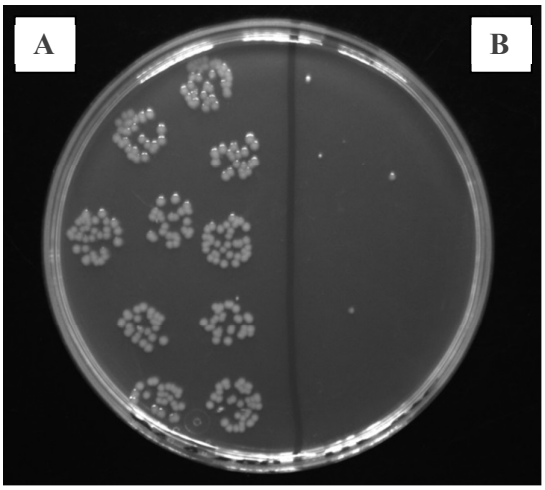

Fig. 6

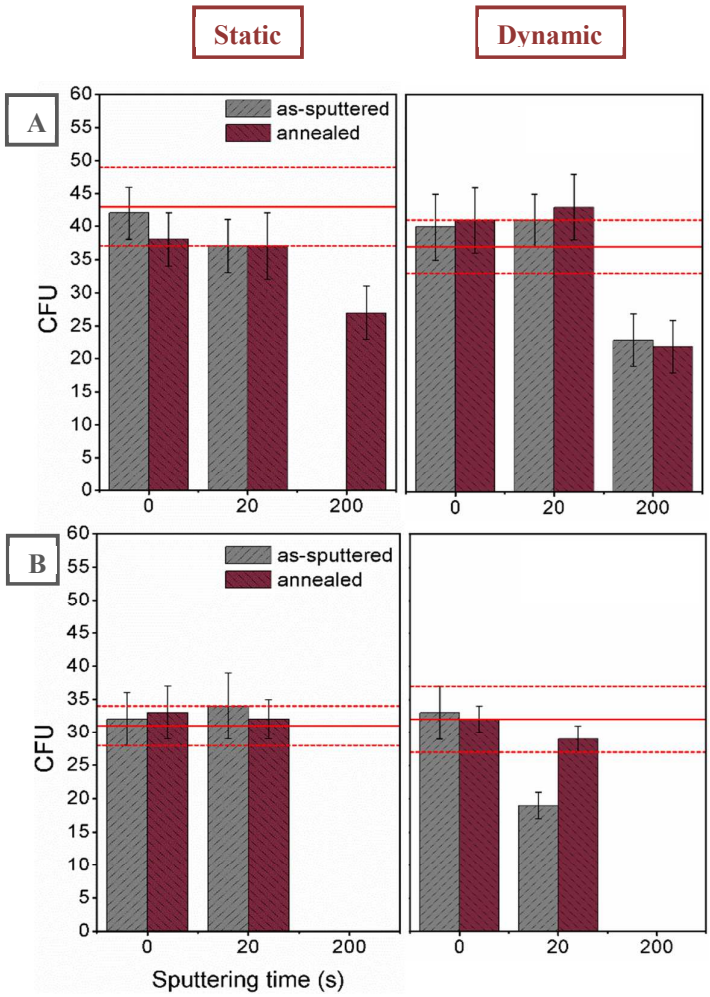

Fig. 7

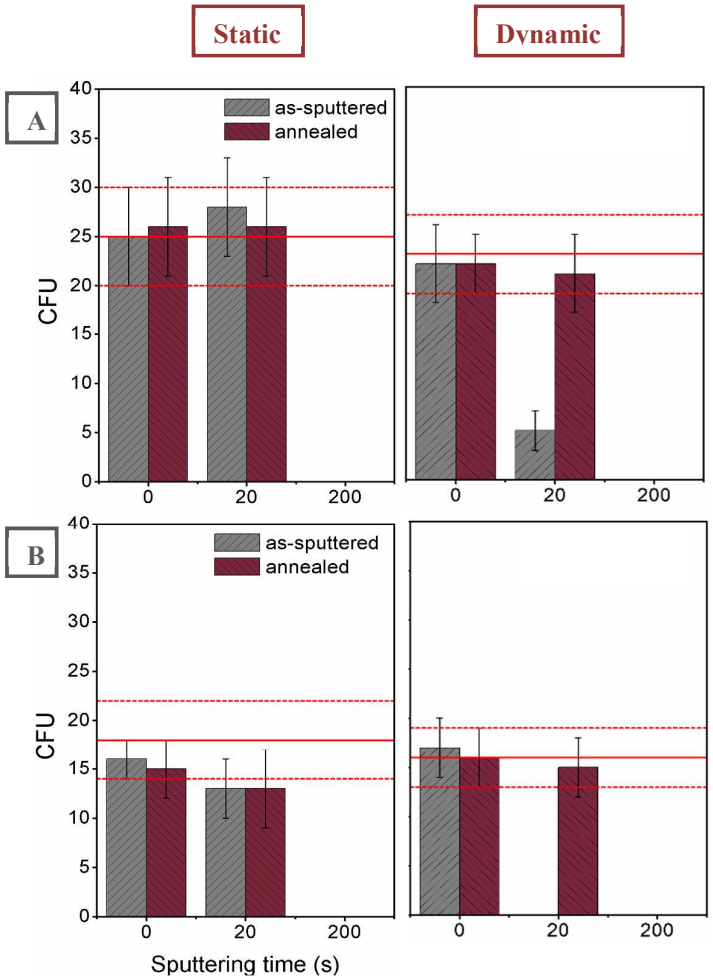

Fig. 8